

## Proton Affinities of Organocatalysts Derived from Pyridine *N*-oxide<sup>†</sup>

Jiří Váňa,<sup>a</sup> Jana Roithová,<sup>a,\*</sup> Martin Kotora,<sup>a,b</sup> Pavel Beran,<sup>b</sup>  
Lubomír Rulíšek,<sup>b,\*</sup> and Pavel Kočovský<sup>a,b</sup>

<sup>a</sup>Department of Organic Chemistry, Charles University in Prague, Hlavova 8, 12843 Prague 2, Czech Republic

<sup>b</sup>Institute of Organic Chemistry and Biochemistry, Academy of Sciences of the Czech Republic, Flemingovo náměstí 2, 166 10 Prague 6, Czech Republic

RECEIVED MARCH 27, 2014; REVISED MAY 2, 2014; ACCEPTED JUNE 9, 2014

**Abstract.** Proton affinities of several efficient organocatalysts METHOX, QUINOX, ANETOX, KOTOX, FUREOX, and FUROOX bearing a pyridine *N*-oxide or 2,2'-bipyridyl *N,N'*-dioxide moiety were determined by using extended kinetic method and density functional theory calculations. Proton affinities are in the range of 1030–1060 kJ mol<sup>-1</sup>. Using isodesmic reactions, the effect of combining two pyridine *N*-oxide units in the neutral and the protonated molecule was studied: The combination of an unfavorable interaction in the former case and a favorable interaction in the latter accounts for the superbasic properties of 2,2'-bipyridyl *N,N'*-dioxides. Last but not least, the theoretically predicted p*K*<sub>a</sub> in ethanol are 0.1, –2.7, 0.9, 1.8, 1.9, and 2.3 for the METHOX, QUINOX, ANETOX, FUROOX, FUREOX, and KOTOX, respectively.

**Keywords:** density functional theory, isodesmic reactions, kinetic method, mass spectrometry, organocatalysis, proton affinity, superbases

### INTRODUCTION

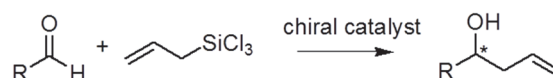
Investigation of strong organic bases (superbases) represents an interesting academic topic.<sup>1–5</sup> Development of new superbases is usually based on two approaches. One can either conceive molecules with a potential of very efficient delocalization of the positive charge over a large molecular scaffold or alternatively, molecules with more than one highly basic functions cooperating in binding of the proton can be considered. As an example of the first approach, the phenylene bis-guanidines developed by Z. Maksić and coworkers<sup>6–11</sup> can be mentioned. A prototypical representative of the second group is *N,N,N',N'*-tetramethyl-1,8-naphthalenediamine, conveniently denoted as proton sponge.<sup>12</sup>

The basic sites of superbases can be used not only for binding of a proton, but can also be employed in catalysis for activation of an electrophilic site. Examples of using strong organic bases as catalysts can be found in the field of organocatalysis.<sup>13</sup> Quite naturally, these two properties of superbases are inherently linked to each other.

In this work, we investigate a series of molecules containing a pyridine *N*-oxide moiety.<sup>14,15</sup> These molecules

have been used as Lewis basic catalytic activators of allyltrichlorosilane for addition to aldehydes (Scheme 1). It has been shown previously that catalysts derived from the axially chiral 2,2'-bipyridyl *N,N'*-dioxide or 2-aryl pyridine *N*-oxide are very efficient as catalysts of the reaction shown in Scheme 1 providing both high yields and high enantioselectivities.<sup>16–20</sup>

By combination of an extended kinetic method and theoretical calculations we aimed at determining the gas-phase proton affinities of a series of organocatalysts employed in the allylation reaction (Chart 1) and theoretical values of their acidity constants in solution (p*K*<sub>a</sub>). Recently, we have shown that molecules derived from 2,2'-bipyridyl *N,N'*-dioxide have very large proton affinities (1050–1070 kJ mol<sup>-1</sup>) in the gas phase and can be denoted as superbases.<sup>21</sup> The catalysts examined here can be divided into two different classes according to their structure. The ANETOX, KOTOX, FUREOX and



**Scheme 1.** Enantioselective allylation of aldehydes

<sup>†</sup> Dedicated to Dr. Mirjana Eckert-Maksić on the occasion of her 70<sup>th</sup> birthday.

\* Authors to whom correspondence should be addressed. (E-mail: roithova@natur.cuni.cz; lubomir.rulisek@uochb.cas.cz)

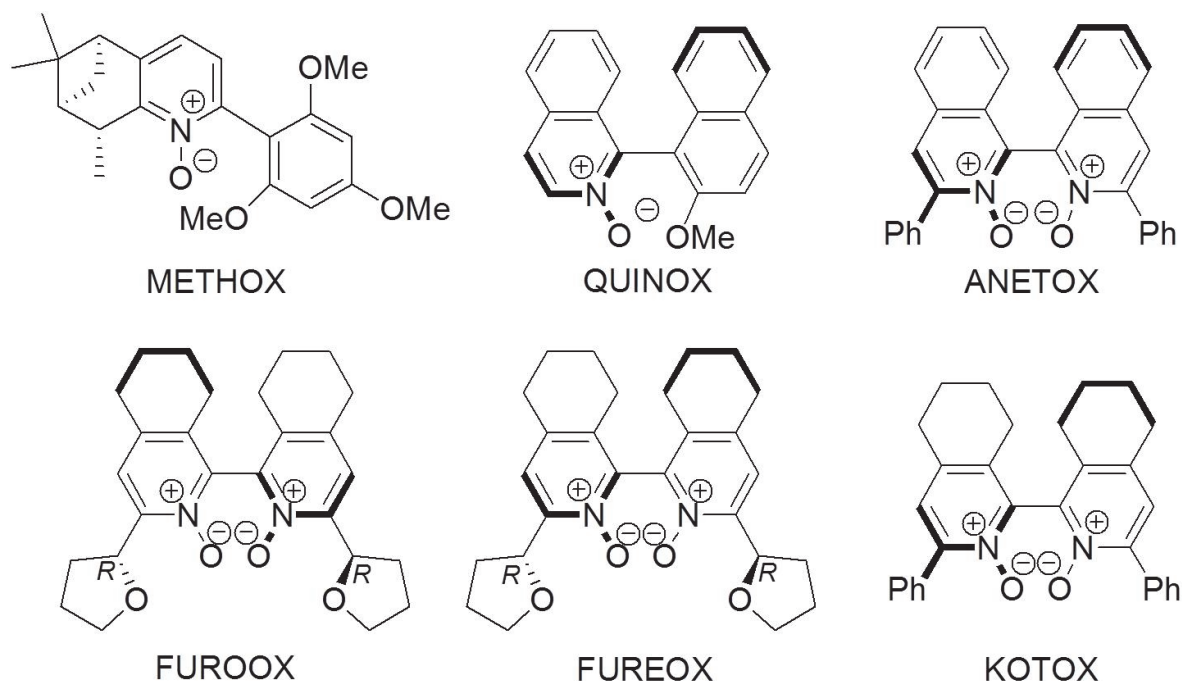


Chart 1.

FUROOX are 2,2'-bipyridyl *N,N'*-dioxide derivatives, whereas QUINOX and METHOX contain only one pyridine *N*-oxide moiety.

## EXPERIMENTAL

The catalysts were prepared by us previously.<sup>16,17</sup> The experiments were performed with a TSQ Classic mass spectrometer equipped with an electrospray ion source and a QOQ configuration of the manifold (Q stands for quadrupole and O for octopole). Mixing millimolar amounts of catalysts with reference bases – DIPEA (diisopropylamine), TPA (tripropylamine), TBA (tributylamine), TEA (triethylamine) and DMAN (*N,N,N',N'*-Tetramethyl-1,8-naphthalenediamine) in methanol (HPLC quality) lead to the formation of mixed proton-bound complexes of the structure  $[A-H-B]^+$  where A stands for the catalyst and B for the reference base. The capillary temperature was set to 250 °C and the ion source was operated under reasonably soft ionization conditions favoring the formation of proton-bound dimers. These  $(A-H-B)^+$  were mass-selected by Q1 and collided with xenon at pressures of typically  $7 \cdot 10^{-5}$  mbar. The collision energy was adjusted by changing the offset between Q1 and O, while the offset of Q2 was locked to the sum of the offsets of Q1 and O. The zero-point of the kinetic energy scale as well as the width of the kinetic energy distribution (FWHM =  $1.1 \pm 0.1$  eV) were determined by means of retarding-potential analysis. The ionic fragments ( $AH^+$  and  $BH^+$ ) emerging from the octopole were detected by Q2 and the respective abun-

dances were determined by using a Daly-type detector operated in the counting mode. The collision energy was changed in steps of 0.25 eV (in the laboratory frame) and 30 scans were accumulated to achieve a good signal-to-noise ratio in the resulting branching ratio.

## Computational Details

The quantum chemical calculations reported in this work were performed using the TURBOMOLE 6.5<sup>22</sup> and Gaussian 09<sup>23</sup> programs. The geometry optimizations were carried out at the DFT level employing the density-fitted (vide infra) Perdew-Burke-Ernzerhof (PBE) functional<sup>24</sup> in conjunction with Grimme's D3 empirical dispersion correction<sup>25</sup> (RI-DFT+D3 method) and the def2-SVP basis set on all atoms.<sup>26,27</sup> The reported single-point energies were obtained using B3LYP<sup>28</sup> and PBE functionals (with and without the D3 correction); the 6-311++G(2d,p) and the def2-TZVP<sup>29</sup> basis sets were employed. The calculations were expedited by expanding the Coulomb integrals in an auxiliary basis set, using the resolution-of-identity (RI) approximation (density-fitting).<sup>30</sup>

Prior to calculating the thermodynamic quantities and solvation energies, conformational search was performed for each structure manually. It consisted in testing several conformers (2–10) for each studied compound. We presume that the reported equilibrium geometries should be very close to the global energetic minima of the studied molecules.

Solvation (free) energies of all studied species were calculated using the COSMO-RS method<sup>31,32</sup>

(conductor-like screening model for realistic solvation) as implemented in the COSMOtherm program,<sup>33</sup> using the “BP\_TZVP\_C30\_1201.ctd” parametrization file. The geometries in solvent (acetonitrile,  $\epsilon = 35.7$ ) were first optimized using the Becke-Perdew (B-P86) functional<sup>34,35</sup> and the COSMO implicit solvation model.<sup>36</sup> The COSMO-RS calculations were then carried out according to the recommended protocol, which includes the RI-BP86/def-TZVP calculations with  $\epsilon = \infty$  (ideal conductor) or  $\epsilon = 1$  (vacuum) as a prerequisite for final calculations in the target solvent (dichloromethane, acetonitrile, and water). The Gibbs free energy was then calculated as the sum of the following contributions:

$$G = E_{\text{el}} + G_{\text{sol}} + E_{\text{ZPVE}} + pV - RT \ln(q_{\text{trans}} q_{\text{rot}} q_{\text{vib}}), \quad (1)$$

where  $E_{\text{el}}$  is the *in vacuo* energy of the system (at the DFT(B3LYP+D3)/def2-TZVP//RI-PBE+D3/def2-SVP level). The  $G_{\text{sol}}$  is the solvation free energy, calculated using the RI-BP86/def-TZVP(COSMO-RS,  $\epsilon = 1$ ,  $\epsilon = \infty$ ) method as described above. The zero-point vibrational energy ( $\Delta E_{\text{ZPVE}}$ ), thermal contributions to enthalpy, and entropic contributions were calculated using the analytical harmonic vibrational frequencies obtained at the RI-PBE+D3/def2-SVP level. The standard formulas of statistical thermodynamics corresponding to the ideal-gas, rigid rotor, and harmonic oscillator approximations<sup>37</sup> were then used to obtain thermodynamic functions at  $T = 298$  K and  $p = 1$  atm.

The correction of  $(7.9 \cdot \Delta n)$  kJ mol<sup>-1</sup> (corresponding to the difference between the concentration of the ideal gas at 298 K and 1 atm and its 1 mol l<sup>-1</sup> concentration) has been included in a free energy value corresponding to the solvation of a proton in ethanol. The values of  $\Delta G_{298\text{K}}^{\ominus}(\text{H}^+, \text{ethanol}) = 1118$  kJ mol<sup>-1</sup> derived from our previous work<sup>38</sup> was used.

## RESULTS AND DISCUSSION

The proton affinities of the selected organocatalysts (A) in the gas phase were determined by employing the extended kinetic method (Figure 1).<sup>39–41</sup> A series of known reference bases (B) with known proton affinities was used and their competition for a proton with the studied organocatalysts then yielded the proton affinities of the studied compounds. The reference bases included proton sponge (DMAN = *N,N,N',N'*-Tetramethyl-1,8-naphthalenediamine), diisopropylethylamine (DIPEA), tributylamine (TBA), tripropylamine (TPA), and triethylamine (TEA). For each of these bases and a given organocatalyst A, gaseous proton-bound dimers [A–H–B]<sup>+</sup> were generated by electrospray ionization of their methanolic solution and their dissociation was studied. The prerequisite for the determination of proton affinities is an exclusive fragmentation of [A–H–B]<sup>+</sup> to AH<sup>+</sup> + B or

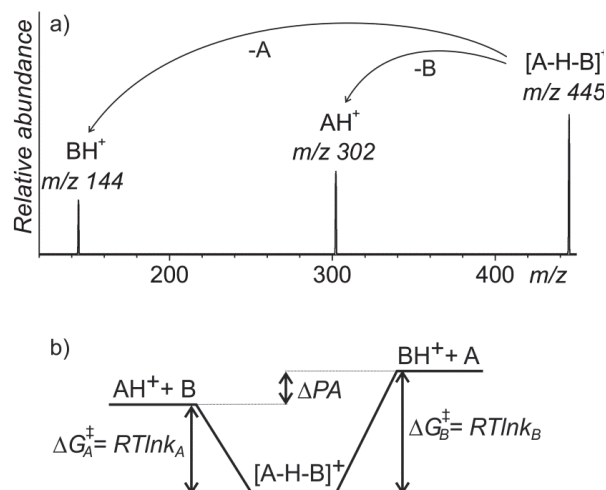


**Figure 1.** Collision induced dissociation spectrum of mass-selected proton-bound dimers [A–H–B]<sup>+</sup>,  $m/z$  445, where A is QUINOX and B is tripropylamine,  $m/z$  144 (a). Principle of the kinetic method for the determination of proton affinities (b).

A + BH<sup>+</sup>, which is fulfilled for all bases studied here (e.g., Figure 1a).

It is assumed that the relative abundances of AH<sup>+</sup> and BH<sup>+</sup> depend on the dissociation rates of the cluster [A–H–B]<sup>+</sup> according to the equation:

$$\ln\left(\frac{I_{\text{AH}^+}}{I_{\text{BH}^+}}\right) \approx \ln\left(\frac{k_{\text{A}}}{k_{\text{B}}}\right) \approx \frac{GB_{\text{A}} - GB_{\text{B}}}{RT_{\text{eff}}} \approx \frac{PA_{\text{A}} - PA_{\text{B}}}{RT_{\text{eff}}} \quad (2)$$

where  $GB$  stands for the gas-phase basicity,  $PA$  is the proton affinity and  $T_{\text{eff}}$  is an effective temperature.

In the simple scheme shown in Figure 1, it is assumed that the dissociation of the proton-bound dimer is an endothermic barrier-less process. While this condition is fulfilled for a complex of the [Cl–H–Br]<sup>+</sup> type, we may expect that for the bases studied here the dissociation process will be complicated by geometry changes and these can be particularly substantial for bidentate bases. Hence, the value determined for A from dissociations of [A–H–B]<sup>+</sup> does not correspond directly to proton affinity of A, but includes also an unknown entropic contribution. Hence, it is denoted as “apparent gas-phase basicity” ( $GB_{\text{app}}$ ). The entropy contribution depends on the temperature ( $\Delta GB_{\text{app}}^T = \Delta PA^T + T\Delta S$ ), which is in the experiment determined mainly by the collision energy (Figure 2a). Therefore, the apparent gas-phase basicities need to be determined at different collision energies (*i.e.*, temperatures) and their temperature dependence is extrapolated to  $T = 0$  K (Figure 2b). This procedure leads to a proton affinity that does not include the entropy part ( $PA^{0\text{K}}$ ).

The entropy effects are substantial for all bases studied here. As an illustration, Figure 3 shows the

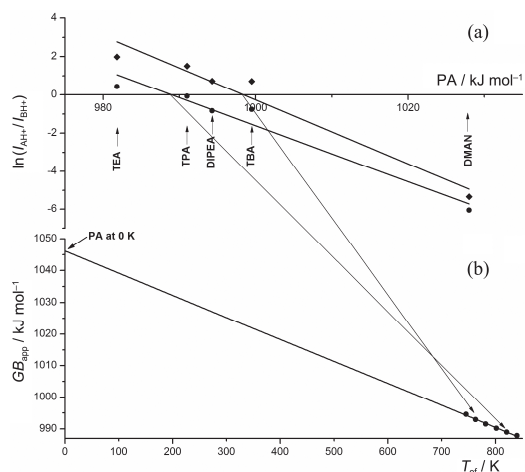


**Figure 2.** Determination of proton affinity of ANETOX using the extended kinetic method. Determination of gas-phase basicity of ANETOX at collision energies 3 eV (diamonds) and 4.5 eV (circles), respectively, by linear fits of the dependences of  $\ln(I_{\text{AH}^+}/I_{\text{BH}^+})$  as a function of the  $PA$  of the reference base B. The intersection of a given linear fit with the  $x$ -axis gives  $GB_{\text{app}}(\text{ANETOX})$ . The effective temperature corresponding to a given collision energy is determined from the slope of the linear fit (a). The dependence of  $GB_{\text{app}}(\text{ANETOX})$  on the effective temperature. The extrapolations of the linear fits of the data obtained at  $E_{\text{CM}}$  2.5, 3.0, 3.5, 4.0, 4.5, and 5.0 eV to  $T_{\text{eff}} = 0$  K gives the estimations of  $PA_{\text{exp}}^{0\text{K}}$  (b).

dependences of  $\ln(I_{\text{BH}^+}/I_{\text{AH}^+})$ , where A are the organocatalysts studied here and B is reference amine DIPEA. Clearly, dramatic changes in fragmentation behavior can be observed at very low collision energies. In order to minimize errors of the measurements, we fitted these dependencies by the exponential functions and obtained the corresponding values of  $\ln(I_{\text{AH}^+}/I_{\text{BH}^+})$  at  $E_{\text{CM}}$  2.5, 3.0, 3.5, 4.0, 4.5, 5.0 eV (see the Supporting Information). These values were further used for determination of the proton affinities. In the first step, the ratios were plotted against  $PA$ s of the reference bases (*cf.* Figure 2a). The intersects of the linear fits of these dependencies with the  $x$ -axis give values of  $GB_{\text{app}}$  and their slopes correspond to  $1/RT_{\text{eff}}$  at given  $E_{\text{CM}}$ . Extrapo-

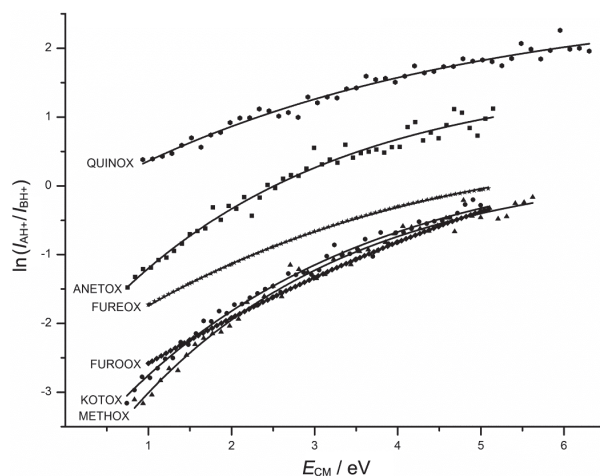


**Figure 3.** The comparison of  $\ln(I_{\text{BH}^+}/I_{\text{AH}^+})$  for individual catalyst with the reference base DIPEA (diisopropylethylamine).

lation of the dependence of  $GB_{\text{app}}$  on  $T_{\text{eff}}$  to  $T_{\text{eff}} = 0$  K gives  $PA_{\text{exp}}^{0\text{K}}$  (Figure 2b). The correction of proton affinities to the temperature of 298 K was then taken from theoretical calculations. Hence, the term  $PA_{\text{theor}}^{298\text{K}} - PA_{\text{theor}}^{0\text{K}}$  was added to the experimental  $PA_{\text{exp}}^{0\text{K}}$  to give the final  $PA_{\text{exp}}^{298\text{K}}$ . The final results for all organocatalysts subjected to this analysis are summarized in Table 1.

The proton affinities for all studied systems were also calculated theoretically as the difference in the standard enthalpies,  $\Delta H_0(T)$ , between the neutral and protonated form. To compare theory with the experiment, the temperatures  $T = 0$  K and 298 K were considered. The difference between  $PA^{0\text{K}}$  and  $PA^{298\text{K}}$  is essentially equal to  $5/2RT$  (translational enthalpy of proton, 6.2  $\text{kJ}\cdot\text{mol}^{-1}$  at  $T = 298.15$  K) and an almost negligible contribution originating from the change of the thermal vibrational energy after protonation.

The results are summarized in Table 1 and the equilibrium geometries of protonated forms are depicted in Figure 4. A very good agreement between the experimental and theoretical  $PA$ s has been found by using B3LYP+D3/def2-TZVP model chemistry (standard deviation between experimental and calculated values is

**Table 1.** The experimental and theoretical  $PA$  values (expressed in  $\text{kJ}\cdot\text{mol}^{-1}$ )

Catalyst	$PA_{\text{exp}}^{0\text{K}}$	$PA_{\text{exp}}^{298\text{K}}$	$PA_{\text{th}}^{0\text{K}}$		$PA_{\text{th}}^{298\text{K}}$	
			B3LYP-D3 <sup>(a)</sup>	B3LYP <sup>(a)</sup>	B3LYP <sup>(a)</sup>	PBE-D3 <sup>(a)</sup>
METHOX	1048 ± 1.5	1055 ± 1.5	1040	1047	1037	1023
QUINOX	1032 ± 1.3	1039 ± 1.3	1010	1017	1006	990
ANETOX	1046 ± 2.3	1053 ± 2.3	1043	1050	1041	1028
FUROOX	1049 ± 0.6	1055 ± 0.6	1047	1053	1048	1038
FUREOX	1039 ± 1.3	1045 ± 1.3	1049	1055	1051	1040
KOTOX	1059 ± 3.4	1065 ± 3.4	1055	1061	1054	1043

<sup>(a)</sup> Basis set: def2-TZVP

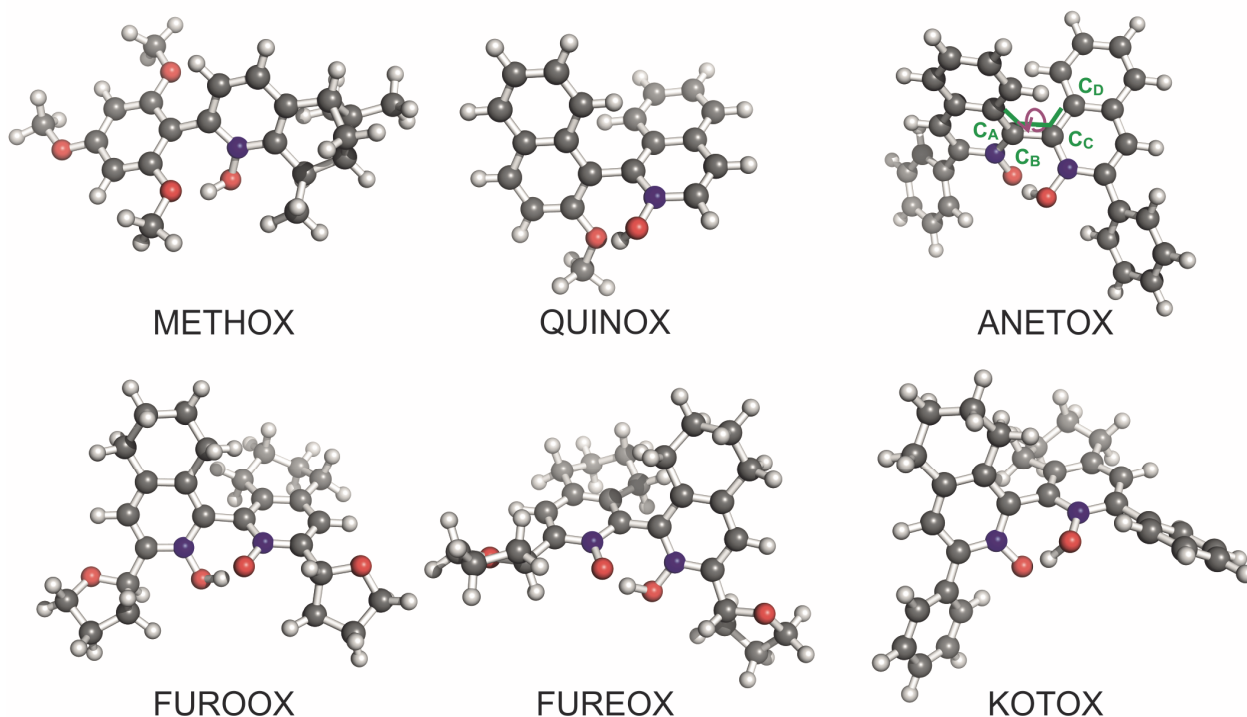


**Figure 4.** Equilibrium molecular geometries of the protonated forms of the organocatalysts.

10 kJ mol<sup>-1</sup>. The agreement for other tested functionals (PBE, TPSS), as well as for the MP2 method, was slightly worse (for comparison, the PBE+D3/def2-TZVP and B3LYP/def2-TZVP are shown in Table 1 as well). In all cases the calculated values mostly suffered from systematic shifts, but the relative proton affinities were predicted correctly (data not shown). It can be mentioned that the dispersion correction (D3) lead to only small systematic shifts in the calculated values, in the range of 0–4 kJ mol<sup>-1</sup> in the  $PA^{0K}$  with the upper limit (3–4 kJ mol<sup>-1</sup>) pertinent to QUINOX and METHOX (*N*-monooxides).

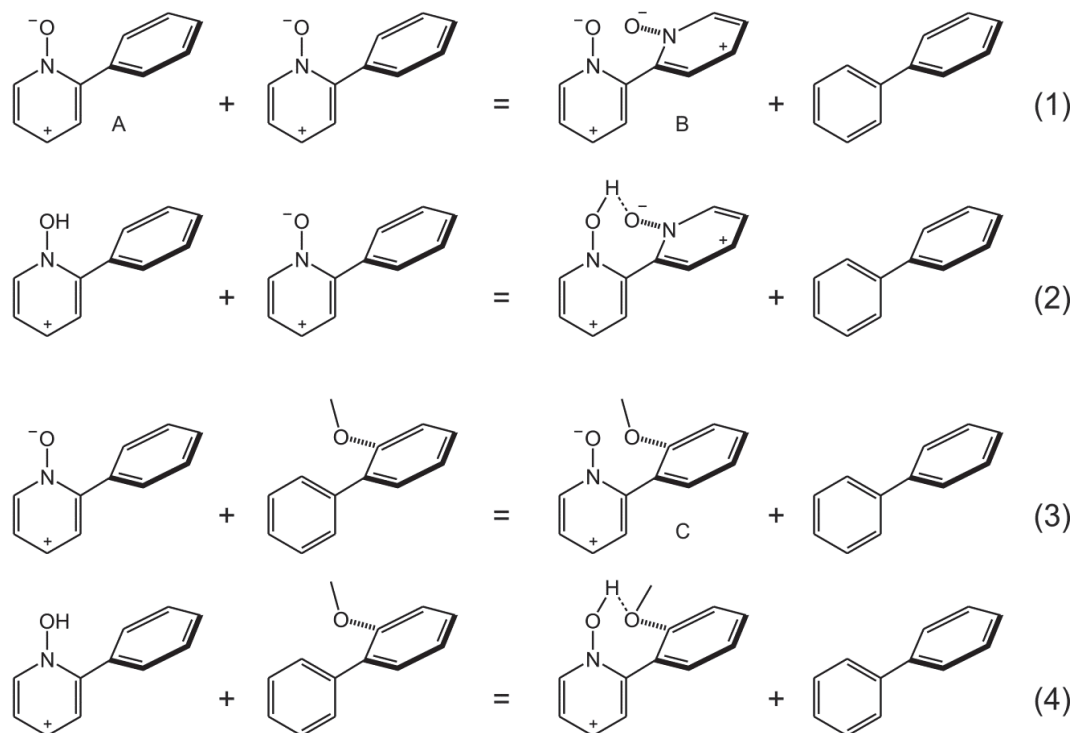
In the case of the best performing functional - B3LYP+D3 - the experimental values are underestimated by 2–8 kJ mol<sup>-1</sup> with the exception of FUREOX, for which an overestimation of 10 kJ mol<sup>-1</sup> has been found. However, the significant and remarkable difference between the experimental and theoretical data was observed for QUINOX, where a discrepancy of 22 kJ mol<sup>-1</sup> sticks out from the otherwise very good correlation between theory and experiment. At present we do not have any explanation for this discrepancy.

As can be seen in Figure 4, the proton is always shared between two *N*-oxide groups in the case of bipyridyl *N,N'*-dioxides or between the *N*-oxide group and the adjacent methoxy group in the case of pyridine *N*-oxides. An interesting geometrical parameter to ana-

lyze is the tilt between the two aromatic rings forming the core of the molecules, defined as the  $C_A-C_B-C_C-C_D$  dihedral angle (where  $C_B$  and  $C_C$  are the linking carbon atoms; cf. Figure 4), and its change upon protonation. This dihedral angle also loosely corresponds to the dihedral angle between the two *N*-oxide units (or the *N*-oxide and methoxy group in the case of QUINOX and METHOX).

For ANETOX, METHOX, and QUINOX this change is almost identical and amounts to 11.3, 11.1, and 11.2 degrees, respectively (in the direction of the co-planarization of these two covalently bound aromatic rings. For the KOTOX, FUROOX, and FUREOX, the change in tilt of the two rings is larger and amounts to 41.4, 52.3, 52.1 degrees, respectively. It is a consequence of the fact that the *N*-oxide groups in the neutral (non-protonated) forms are located far apart (dihedral greater than 90 degrees). In fact, the dihedral angle of the crystalline METHOX was found to be 115°, as revealed by X-ray crystallography.<sup>20</sup> Quite surprisingly, there is no correlation between the proton affinity and the above geometrical parameter and it is therefore the different electronic structure of the individual systems that primarily determines the proton affinity (*vide infra*).

Both experimental and theoretical results clearly show that KOTOX has the largest proton affinity from all these molecules (1059 kJ mol<sup>-1</sup> determined experi-



Scheme 2. Isodesmic reactions

mentally and 1055 kJ mol<sup>-1</sup> computed theoretically). The origin of its basicity was studied before.<sup>21</sup> It was shown that both annulated cyclohexyl rings as well as the phenyl substituents stabilize the positive charge in the protonated molecule.<sup>21</sup> The replacement of the phenyl substituents with tetrahydrofuryl groups leads to a decrease of proton affinity by ca 10–20 kJ mol<sup>-1</sup> (FUROOX and FUREOX), both according to the calculations and experiment. Similarly, aromatization of the rings condensed to the pyridine *N*-oxide moiety leads to a decrease of proton affinity by ~13 kJ mol<sup>-1</sup> (ANETOX).

As discussed above, one would expect that the proximity of two pyridine *N*-oxide moieties in KOTOX, FUROOX, FUREOX, and ANETOX should provide a cooperative effect on proton affinity and therefore a substantial drop of the proton affinity could be expected if one of the *N*-oxide groups is removed. Surprisingly, METHOX and QUINOX still show very high proton affinities: thus, the proton affinity of METHOX is comparable to those of FUROOX and ANETOX. The origin of the large proton affinity of METHOX can be identified in the condensed aliphatic ring which will provide stabilization of the positive charge of the protonated

**Table 2.** Reaction enthalpies of reactions (1)–(4) (expressed in kJ mol<sup>-1</sup>) and proton affinities of A, B, and C (see Scheme 2); where A = 2-phenylpyridine *N*-oxide, B = 2,2'-bipyridyl *N,N'*-dioxide, and C = (2-methoxyphen-1-yl)pyridine *N*-oxide

Reaction	B3LYP/6–311+G**			B3LYP-D3/6–311+G**		
	$\Delta H_{\text{rxn}}^{0\text{K}}$	$\Delta H_{\text{rxn}}^{298\text{K}}$	$\Delta G_{\text{rxn}}^{298\text{K}}$	$\Delta H_{\text{rxn}}^{0\text{K r}}$	$\Delta H_{\text{rxn}}^{298\text{K}}$	$\Delta G_{\text{rxn}}^{298\text{K}}$
1	4.9	5.3	8.3	6.3	6.6	10.0
2	-48.7	-51.0	-41.3	-46.1	-48.5	-38.4
3	-3.9	-3.8	-0.7	-4.1	-3.9	-1.5
4	-43.5	-45.3	-36.0	-44.1	-46.0	-36.6
Base	$PA^{0\text{K}}$	$PA^{298\text{K}}$		$PA^{0\text{K r}}$	$PA^{298\text{K}}$	
A	950	948		953	951	
B	1004	1005		1005	1006	
C	990	990		993	993	

molecule by an inductive effect. Moreover, the protonated *N*-oxide moiety can be stabilized by the interaction with the methoxy group of the aromatic substituent. Proton affinity of QUINOX is the lowest within all the values determined here, as could be expected from the structure of its molecule.

The cooperative effect of the two *N*-oxide functions and the effect of the methoxy group was further analyzed by using isodesmic reactions depicted in Scheme 2. Reaction enthalpies of the isodesmic reactions (1)–(4) describe how the bringing of two functionalities (either two *N*-oxide functions, or the *N*-oxide function with the methoxy group) to their mutual vicinity stabilizes or destabilizes the neutral molecule or its protonated form.<sup>42,43</sup> The reference molecule is 2-phenylpyridine *N*-oxide, which is in a Gedankenexperiment stabilized or destabilized by introducing the *N*-oxide moiety or the methoxy group to the phenyl substituent.

Reaction enthalpies of the isodesmic reactions (Table 2) show that while the introduction of the methoxy group is stabilizing both the neutral and the protonated form, the second *N*-oxide moiety is stabilizing only the protonated form (the respective isodesmic reactions are exothermic). The non-favorable interaction of two *N*-oxide functions can be simply understood, because it is associated with the direct C–C binding of two partially positively charged aromatic rings. When we analyze the magnitude of the effects at the B3LYP level of theory, the protonated forms are by  $\sim 5$  kJ mol<sup>-1</sup> more stabilized by the second *N*-oxide function than by the methoxy substituent. In the neutral forms, the difference is  $\sim 9$  kJ mol<sup>-1</sup> and has the opposite direction (the methoxy group slightly stabilizes, whereas the *N*-oxide function destabilizes as explained above). The combination of these effects explains the large proton affinities found for the derivatives of 2,2'-bipyridyl *N,N'*-dioxides and suggests that the bases derived from (2-methoxyphen-1-yl)pyridine *N*-oxide should have about 14 kJ mol<sup>-1</sup> lower proton affinities if other substituent effects do not play a role.

Comparison of the results obtained with the plain B3LYP functional and the results containing correction of the dispersion interactions show interesting effects. Including dispersion interactions in the theoretical description of 2,2'-bipyridyl *N,N'*-dioxide makes the interaction of the two pyridyl *N*-oxide groups by  $\sim 2$  kJ mol<sup>-1</sup> less favorable. The effect is almost identical for both the neutral and protonated form. Therefore, no significant effect (with respect to the reference compound pyridine *N*-oxide) should be observed during calculations of *PAs* (as shown above). For (2-methoxyphen-1-yl)pyridine *N*-oxide are the effects again very similar for the neutral and the protonated form, but this time the effect of dispersion interactions is slightly stabilizing. Nevertheless, the resulting *PAs* are again with respect to the reference compound pyridine *N*-oxide almost unchanged.

Finally, we have utilized the calculated values of proton affinities in calculations of the acidity constants in ethanol, using the COSMO-RS solvation model for the calculations of solvation free energies. It was shown previously<sup>44,45</sup> that this protocol often yields theoretical values that are within 1 p*K*<sub>a</sub> unit accuracy. The theoretically predicted p*K*<sub>a</sub> in ethanol are 0.1, -2.7, 0.9, 1.8, 1.9, and 2.3 for the METHOX, QUINOX, ANETOX, FUREOX, FUREOX, and KOTOX, respectively (using the B3LYP+D3 *in vacuo* energies and COSMO-RS solvation energies). Calculation of the p*K*<sub>a</sub> of pyridine *N*-oxide in ethanol by using the same protocol gave the value of -1.3. For comparison, experimental p*K*<sub>a</sub> of pyridine *N*-oxide in water is known to be 0.8.<sup>46</sup> It can be seen that the calculated p*K*<sub>a</sub> values correlate well with the calculated proton affinities. Apparently, change in solvation Gibbs energy in ethanol upon protonation of the base is similar along the series. Indeed, the calculated  $\Delta\Delta G_{\text{solv}}(\text{neutral, protonated}) = 21.7\text{--}23.6$  kcal mol<sup>-1</sup> for all compounds except QUINOX (the weakest base) for which it amounts to 27.7 kcal mol<sup>-1</sup>) and partially compensates for the lowest gas-phase proton affinity. This might not be surprising since in all structures intramolecular hydrogen bond is established upon protonation. Therefore partial internal solvation shields the proton from the solvent in all structures.

The high basicities may qualify these organocatalysts derived from pyridine *N*-oxide and 2,2'-bipyridine *N,N'*-dioxide as potential candidates for the matrix-assisted ionization/laser desorption (MAILD) matrices used for metabolomics.<sup>38,44</sup> It is pertinent to note that MAILD is a new technique in mass spectrometry that complements the standard MALDI technique. Nevertheless, the performance of the pyridine *N*-oxide matrices would be probably lower than that of the 1,14-diaza[5]helicene,<sup>47</sup> which has been recently shown to be an optimal matrix.<sup>38</sup>

## CONCLUSIONS

Proton affinities and acidity constants (p*K*<sub>a</sub>) for several organocatalysts based on pyridine *N*-oxide and 2,2'-bipyridyl *N,N'*-dioxide moiety were determined, both experimentally and computationally. It was shown that all the investigated molecules are very strong bases with *PAs* ranging between 1030–1060 kJ mol<sup>-1</sup>. Using density functional theory calculations, we have shown that the origin of high proton affinities of molecules containing 2,2'-bipyridyl *N,N'*-dioxide subunit is a combination of an unfavourable interaction of the two pyridine *N*-oxide units in the neutral form and the cooperative effect of the two *N*-oxide functions in the protonated form. Our data not only serve as reference points in the experimental measurements of proton affinities of various organic molecules, but also provide invaluable information for the quest for new types of superbases that can be utilized, for example, in metabolomics.

**Acknowledgements.** The authors gratefully acknowledge financial support from the European Research Council (StG ISORI) and the Grant agency of the Czech Republic (project 14-31419S and P207/11/0587).

## REFERENCES

- V. Štrukil, I. Đilović, D. Matković-Čalogović, J. Saame, I. Leito, P. Sket, J. Plavec, and M. Eckert-Maksić *New J. Chem.* **36** (2012) 86–96.
- T. Ishikawa, *Superbases for Organic Synthesis*, Wiley, Hoboken, 2009.
- Z. Glasovac, F. Pavošević, V. Štrukil, M. Eckert-Maksić, M. Schlangen, and R. Kretschmer *Int. J. Mass Spectrom.* **354–355** (2013) 113–122.
- M. Eckert-Maksić, Z. Glasovac, P. Trošelj, A. Kutt, T. Rodima, I. Koppel, and I. A. Koppel *Eur. J. Org. Chem.* **30** (2008) 5176–5184.
- A. Tintaru, J. Roithova, D. Schröder, L. Charles, I. Jušinski, Z. Glasovac, and M. Eckert-Maksić *J. Phys. Chem. A* **112** (47) (2008) 12097–12103.
- Z. B. Maksić and B. Kovačević *J. Org. Chem.* **65** (2000) 3303–3309.
- V. Raab, K. Harms, J. Sundermeyer, B. Kovačević, and Z. B. Maksić *J. Org. Chem.* **68** (2003) 8790–8797.
- A. Singh, B. Ganguly *New J. Chem.* **32** (2008) 210–213.
- M. P. Coles, P. J. Aragon-Saez, S. H. Oakley, P. B. Hitchcock, M. G. Davidson, Z. B. Maksić, R. Vianello, I. Leito, I. Kaljurand, and D. C. Apperley *J. Am. Chem. Soc.* **131** (2009) 16858–16868.
- Z. Glasovac, P. Trošelj, I. Jušinski, D. Margetić, and M. Eckert-Maksić *Synlett* **24** (19) (2013) 2540–2544.
- Z. Glasovac, M. Eckert-Maksić, and Z. B. Maksić *New J. Chem.* **33** (2009) 588–597.
- R. W. Alder, P. S. Bowman, W. R. S. Steele, and D. R. Winterman *Chem. Commun. (London)* (1968) 723–724.
- S. E. Denmark and G. L. Beutner *Angew. Chem. Int. Ed.* **47** (2008) 1560–1638 and references cited therein.
- Y. Orito and M. Nakajima *Synthesis* **9** (2006) 1391–1401.
- (a) A. V. Malkov and P. Kocovsky *Eur. J. Org. Chem.* **1** (2007) 29–36. (b) P. Kocovsky and A. V. Malkov *Pure Appl. Chem.* **80**, (2008) 953–966.
- R. Hrdina, M. Dracinsky, I. Valterová, J. Hodačová, I. Cisarova, and M. Kotora *Adv. Synth. Catal.* **350** (2008) 1449–1456.
- (a) A. V. Malkov, M. Bell, F. Castelluzzo, and P. Kocovsky *Org. Lett.* **7** (2005) 3219–3222. See also: (b) A. V. Malkov, M. Bell, M. Vassieu, V. Bugatti, and P. Kocovsky *J. Mol. Catal. A* **196** (2003) 179–186. (c) A. V. Malkov, M. Barlog, Y. Jewkes, J. Mikusek, and P. Kocovsky *J. Org. Chem.* **76** (2011) 4800–4804.
- A. V. Malkov, L. Dufková, L. Farrugia, and P. Kocovsky *Angew. Chem. Int. Ed.* **42** (2003) 3674–3677.
- A. V. Malkov, P. Ramirez-Lopez, L. Biedermannova, L. Rulišek, L. Dufkova, M. Kotora, F. Zhu, and P. Kocovsky *J. Am. Chem. Soc.* **130** (2008) 5341–5348.
- A. V. Malkov, S. Stoncius, M. Bell, F. Castelluzzo, P. Ramirez-Lopez, L. Biedermannova, V. Langer, L. Rulišek, and P. Kocovsky *Chem. Eur. J.* **19** (2013) 9167–9185.
- L. Duchackova, A. Kadlcikova, M. Kotora, and J. Roithova *J. Am. Chem. Soc.* **132** (2010) 12660–12667.
- TURBOMOLE V6.5 2013, a development of University of Karlsruhe and Forschungszentrum Karlsruhe GmbH, 1989–2007, TURBOMOLE GmbH, since 2007; available from [www.turbomole.com](http://www.turbomole.com).
- Gaussian 09, Revision A.2, M. J. Frisch *et al.* Gaussian, Inc., Wallingford CT, 2010.
- J. P. Perdew, K. Burke, and M. Ernzerhof *Phys. Rev. Lett.* **77** (1996) 3865–3868.
- S. Grimme, J. Antony, S. Ehrlich, and H. J. Krieg *Chem. Phys.* **132** (2010) 154104.
- F. Weigend and R. Ahlrichs *Phys. Chem. Chem. Phys.* **7** (2005) 3297–3305.
- A. Schäfer, C. Huber, and R. Ahlrichs *J. Chem. Phys.* **100** (1994) 5829–5835.
- (a) A. D. Becke *Phys. Rev. A* **38** (1988) 3098–3100. (b) C. Lee, W. Yang, and R. G. Parr *Phys. Rev. B* **37** (1988) 785–789. (c) A. D. Becke *J. Chem. Phys.* **99** (1993) 5648–5652. (d) P. J. Stephens, F. J. Devlin, M. J. Frisch, and C. F. Chabalowski *J. Phys. Chem.* **98** (1994) 11623–11627.
- A. Schäfer, C. Huber, and R. Ahlrichs *J. Chem. Phys.* **100** (1994) 5829–5835.
- K. Eichkorn, O. Treutler, H. Öhm, M. Häser, and R. Ahlrichs *Chem. Phys. Lett.* **240** (1995) 283–290.
- A. Klamt *J. Phys. Chem.* **99** (1995) 2224–2235.
- A. Klamt, V. Jonas, T. Buerger, and J. C. W. Lohrenz *J. Phys. Chem.* **102** (1998) 5074–5085.
- F. Eckert; A. Klamt COSMOtherm, version C3.0, release 12.01; COSMOlogic GmbH & Co. KG.
- A. D. Becke *Phys. Rev. A* **38** (1988) 3098–3100.
- (a) S. H. Vosko, L. Wilk, and M. Nusair *Can. J. Phys.* **58** (1980) 1200–1211. (b) J. P. Perdew *Phys. Rev. B* **33** (1986) 8822–8824.
- A. Klamt and G. Schuurmann *J. Chem. Soc.-Perkin Trans. 2* (1993) 799–805.
- F. Jensen *Introduction to Computational Chemistry*; John Wiley & Sons: New York, 1999.
- M. Napagoda, L. Rulišek, A. Jancarik, J. Klivar, M. Samal, I. G. Stara, I. Stary, V. Solinova, V. Kasicka, and A. Svatos *ChemPlusChem* **78** (2013) 937–942.
- R. G. Cooks and P. S. H. Wong *Acc. Chem. Res.* **31** (1998) 379–386.
- R. G. Cooks, J. T. Koskinen, and P. D. Thomas *J. Mass Spectrom.* **34** (1999) 85–92.
- L. Drahos and K. Vekey *J. Mass Spectrom.* **38** (2003) 1025–1042.
- O. Exner *J. Phys. Org. Chem.* **12** (1999) 265–274.
- J. Roithova and O. Exner *J. Phys. Org. Chem.* **12** (1999) 265–274.
- R. Shroff, L. Rulišek, J. Doubsky, and A. Svatos *Proc. Natl. Acad. Sci. U. S. A.* **106** (2009) 10092–10096.
- S. Opekar, R. Pohl, P. Beran, L. Rulišek, and P. Beier *Chem. Eur. J.* **20** (2014) 1453–1458.
- H. H. Jaffe and G. O. Doak *J. Am. Chem. Soc.* **77** (1955) 4441–4444.
- For determination of proton affinities of aza-helicenes see: J. Roithova, D. Schröder, J. Misek, I. G. Stara, and I. Stary *J. Mass Spectrom.* **42** (2007) 1233–1237. s